Spatiotemporal Behaviour of Human Persistent Atrial Fibrillation from Long-Duration Recordings

Mahmoud Ehnesh[1], Xin Li[1, 2, 3], Tiago P. Almeida[1, 2], Sidhu Bharat[2], Ibrahim Antoun[2], Nawshin Dastagir[4], P J Stafford[2, 3], G. André Ng[2, 3], Fernando S. Schlindwein[1, 3]

[1]School of Engineering, University of Leicester, Leicester, UK
[2]Department of Cardiovascular Sciences, Glenfield Hospital, Leicester, UK
[3]National Institute for Health Research Leicester Cardiovascular Biomedical Research Centre, Leicester, UK
[4] Massey University, New Zealand

Abstract

Identifying ablation targets in persistent atrial fibrillation (PersAF) remains challenging. This study aims to investigate the spatiotemporal stability of PersAF drivers within 5 min recordings of virtual atrial electrograms (VEGMs). 2048-channel VEGMs (EnSite Array, Abbott) were analysed for 5 patients undergoing substrate-guided ablation. Following QRST subtraction, dominant frequency (DF, 4-10 Hz) and organization index (OI) were identified using fast Fourier transform (4 s windows; 50% overlap). Areas with DF within 0.25 Hz below or equal the maximum out of the 2048 points were defined as the highest DF (HDF). Stable DFs (SDFs) were defined as DF patterns with the highest recurrence over consecutive time windows. Rotors were defined as phase singularities (PSs) with ≥100 ms. The 5 min VEGMs were divided into segments of 30, 60, 90, and 120 s. 2D correlation coefficients (CORR) was used to measure the similarity among maps (SDFs, DF selected by OI>0.3, HDF and Rotors) at different time segments. DF (OI>0.3) density maps were found to have the highest level of similarity over time, followed by Rotors, HDF, and SDFs. DF (OI>0.3) are the most spatially overlapped regions with the SDFs sites. Similarity and spatial overlapping of individual density maps increased with longer segments. There is spatial overlapping between PersAF drivers density maps, therefore investigate regions of overlapping might lead to better identification of substrate targets ablation for PersAF.

1. Introduction.

The mechanisms driving and sustaining atrial fibrillation (AF) remain incompletely understood. However, there are different ablation concepts associated with the mechanism of initiation and the maintenance of AF [1]. It is noteworthy that pulmonary vein isolation (PVI) ablation remains the foundation of ablation of paroxysmal AF (PAF). Nevertheless, for persistent AF (PersAF) patients, PVI alone is not so effective, and repeat procedures often need to be performed [1]. Therefore, non-PV ablation including linear ablation, complex fractionated atrial electrograms (CFAEs) [2], and focal impulse and rotor modulation (FIRM) [3] targeted ablation is frequently employed. However, none of the above is deemed to be effective at eliminating AF consistently [4]. Interestingly, recent studies have established successful driver identification in the course of mapping PersAF in humans [5, 8]. Frequent electrical activity has been suggested as a pivotal characteristic of PersAF drivers. Therefore, high frequency at a specific site during AF could be considered candidates for PersAF drivers [9]. For this reason, areas of high dominant frequency (HDF) have been suggested as important targets for ablation [10]. Also, DF patterns (DFPs) with the highest recurrence provide an insight into PersAF dynamic behaviour, therefore targeting such sources might result in improvements to the catheter ablation outcomes [11]. Likewise, a higher organization index (OI) of virtual atrial electrograms (VEGMs) is an indication of the dominance of the DF peak within its spectrum, thus such a region is associated with clinically relevant AF sources [12]. Furthermore, phase singularity (PS) analysis has been employed in several clinical centres to suggest areas of rotational activity, "rotors" and regions of high rotational content are ablated [7, 13]. However, there is conflicting evidence on the spatiotemporal stability of such PersAF drivers [10, 14].

This study aims to investigate the spatiotemporal stability of PersAF drivers within 5 min recordings of virtual atrial electrograms (VEGMs).

2. Materials and Methods.

2.1 Electrophysiological study.

In this study, five patients underwent a novel global simultaneous stable DFs targeting protocol for first-time substrate-guided catheter ablation guided by three-dimensional (3D) Non-contact mapping (NCM), using a multi-electrode array catheter (MEA) (EnSite Array, Abbott). Ethics approval to conduct the study was obtained

from the local ethics committee and all procedures were performed with informed consent.

Left atrial (LA) dimensional (3D) electro-anatomical mapping (EAM) was performed on each of the patients. Comprehensive atrial geometries were reconstructed using EAM software (EnSite, Abbott) utilizing the ablation catheter. Anatomical landmarks comprising PV Ostia, left atrial appendage (LAA), roof, septum, anterior, PVs, and mitral valve (MV) annulus were identified and marked. Once the mapping was completed, the array remained in a position to avoid any distortion of the reconstructed isopotential maps. Furthermore, 5 minutes of AF signals were recorded employing non-contact arrays (NCAs). A 90-second data segment and 2048 node geometry were transferred into MATLAB from the LA array and target stable DFs areas were detected and subsequently ablated. A post-procedure recording was obtained for up to 5 minutes of VEGMs signals.

2.3 Data Processing

The VEGMs (2048 channels) data were extracted with the EnSite default band-pass filter set between 1 and 150 Hz. No further filtering was applied to the signals to preserve signal integrity and low-frequency components. The VEGMs were sampled at 2034.5 Hz for offline analysis using MATLAB (R2018b, USA). The VEGMs were resampled at 512 Hz using cubic spline interpolation to reduce processing time. Ventricular far-field activity was removed from the recorded VEGMs using a QRST subtraction technique previously described [15].

2.4 Identification of potential PersAF drivers.

After carrying out ventricular cancellation of the VEGMs, using Fast Fourier Transform (FFT) with a Hamming window DF and OI (DF, 4 -10 Hz, within 4 s windows; and 50% overlap between each sequential window) were identified. However, just DF selected by a certain threshold of OI (set at 0.3 [16]): were identified and considered (DF > 0.3 OI). Areas with DF within 0.25 Hz of the absolute maximum out of the 2048 points were defined as the highest DF (HDF). Stable DFs (SDFs) were defined as DF patterns with the highest recurrence over consecutive time windows [11], however, for phase analysis, Hilbert transform was used to generate an analytical signal from which the instantaneous phase of the VEGMs was obtained. Subsequently, the Phase Singularities points (PSs) were identified and detected using the topologic charge technique (TCT), as described in [17]. Rotors were defined as PSs which last for at least 100 ms [18].

The 5 min segments of VEGMs were divided into shorter records of 30, 60, 90, and 120 s. Similarity index 2D correlation coefficients (CORR) was used to measure the similarity among 2D density maps for (DF > 0.3 OI, Rotors, HDF, and SDFs). Figure 1A illustrates the 2D density maps generated to assess the spatiotemporal stability of the selected PersAF drivers. The 2D density maps within each group of 30, 60, 90, and 120 s were compared against each other in relation to the consecutive density map within 300 s of the VEGMs segments as described in the diagram of correlation coefficients comparison steps figure 1 B.
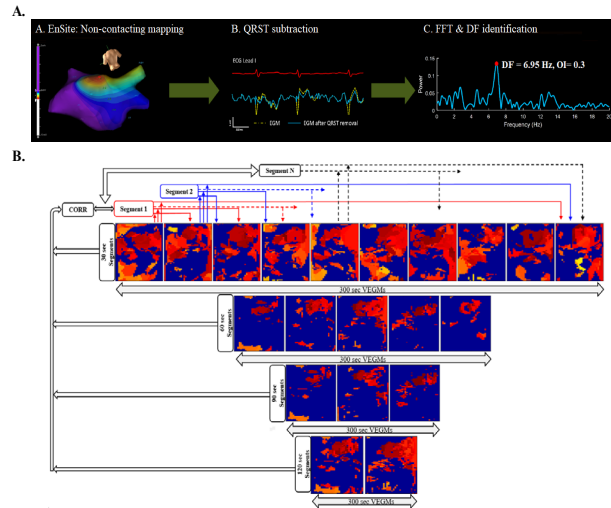

Figure 1(A), A: 3D left atrial geometry generated using EnSite non-contacting mapping system. B; describe the QRST subtraction of VEGMs using one ECG lead as reference. C: illustration of the FFT and DF detection: power spectrum of VEGMs with the annotated DF and OI. (Modified from [11]). (B) Diagram of correlation coefficients comparison steps: the SDFs density maps were used to describe the comparison steps; the 300 s of VEGMs were divided into four groups of 30, 60, 90, and 120 s, ending up with ten density maps for 30 s time duration, five for the 60 s, three for 90 s, and two density maps for the 120 s segment. The comparison was carried out by comparing the first density map of each group to consecutive density maps within the same group and so on so forth, until covering the whole 300 s of VEGMs.

3. Results and Discussions.

3.1 Temporal stability of PersAF drivers.

Figure 2B illustrates the mean of the similarity index for all patients. The results showed that DF (OI>0.3) and Rotors density maps have the highest level of similarity over time, thereby higher temporal stability, followed by HDF and SDFs respectively (table 1).

Table 1: The result of CORR similarity index for all patients

	CORR (Mean ± SD %)			
	30 s	**60 s**	**90 s**	**120 s**
DF > 0.3 OI	28 ±0.4	39 ±0.3	46 ±0.3	56 ±0.1
Rotors	24±0.4	36±0.1	49±0.1	55±0.2
HDF	17 ±0.6	30 ±0.2	31 ±0.1	33 ±0.4
SDFs	13 ±0. 2	16 ±0. 6	12 ±0. 3	19 ±0. 1

Figure 2A suggests that the locations of the dense regions

in DF (OI>0.3), Rotors, and also HDF density maps appeared to remain consistent over consecutive time segments of 300 s of the VEGMs in the all-time duration segments analysed, therefore, these consistent locations of the dense regions could be indicative of stable drivers of PersAF. Whereas, the SDFs results were less stable over 300 s of VEGM recordings. Our finding in relation to the spatiotemporal of PersAF drivers, supports the fact that the concept of ablating single AF driver ablation at the time, for instance, FIRM or CFAEs, should be advocated. Therefore, combining the PersAF drivers ablation strategy might result in improvements to the clinical outcomes for catheter ablation for PersAF. From the results in Figure 2C, it is clear that for all PersAF drivers tested, as time duration increases the similarity among the density maps increases too (Mean ± SD %, the 30s: 21.2 % ±0.7, 60s: 31.5 % ± 0.5, 90s: 32.8 % ±0.1, 120s: 45 % ±0.1). Thus, temporal stability improves. As the processing time required to produce the density map increases with duration of the data records, reducing the duration of the segments is desirable. Our results suggest that using non-contact VEGMs, 60 s segment seems to be sufficient to identify important PersAF drivers in PersAF patients.
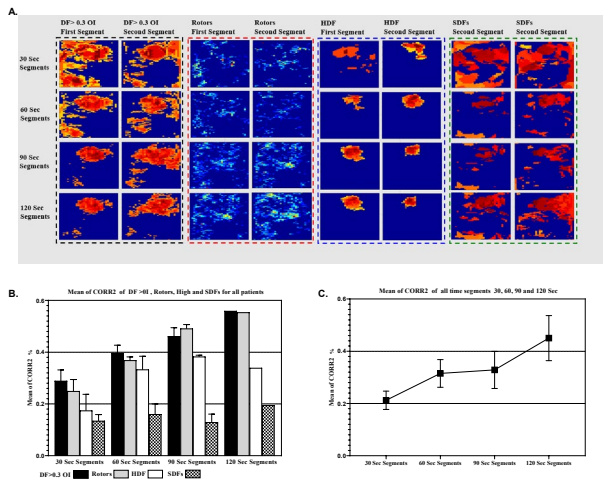

Figure 2(A), Illustrates the results of 2D density maps of the first two consecutive time segments of the PersAF drivers (DF > 0.3 OI, Rotors, HDF, and SDFs) for one patient, where each row represents the time duration segment of 30, 60, 90, and 120 s. (B) Mean of CORR for the AF derivers DF > 0.3 OI, Rotors, HDF, and SDFs. The bar graph illustrates the results of comparing each density map of PersAF drivers against each other in relation to the consecutive density map within 300 s for the time duration as described in figure 1B. Ten density maps for 30 s were compared, five for 60s, three for 90s, and two for the 120 s. (C) Illustrates the result of the mean of CORR for each time duration 30, 60, 90, and 120 s for the PersAF drivers tested.

3.2 Spatial interactions of PersAF drivers regions.

A major debate in studies showing PersAF drivers is whether or not they are spatially stable [9-11]. The present study offers an insight into the spatial overlapping between the PersAF drivers. We created an algorithm to investigate if the dense regions of DF > 0.3 OI, HDF, and Rotors are spatially overlapping with the SDFs sites within the LA since SDFs were the ablation target in this study. To understand their interactions in the co-localisation behaviour of such drivers. For all patients, the results show that there is spatial overlapping between PersAF drivers density maps as following (Figure 3D: Mean ± SD%, DF > 0.3 OI: 21.4 ± 2.1%, HDF: 20.8 ± 0.6%, Rotors: 17 ± 0.2%). The overlapping percentages might appear to be relatively small values, however, considering that overlapping percentage considers the entire size of LA, this finding could potentially indicate common consistent locations of dense regions that might represent the likelihood of individual targets for atrial substrate ablation of PersAF.
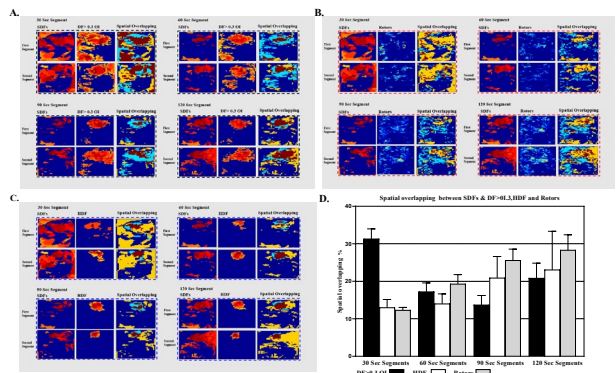

Figure 3 (A), the 2D density maps of two consecutive time segments for one patient for 30, 60, 90 and 120 s segments: The first column is SDFs density maps, and the second column is the DF > 0.3 OI maps and the last column represents the overlapping maps; SDFs are represented with yellow color, DF> 0.3OI with blue, and overlapped areas with brown. (B) Shows the spatial overlapping between SDFs density maps and Rotors density maps for one patient. (C) Shows the spatial overlapping between SDFs density maps and HDF density maps for one patient. (D) Illustrates the percentages of spatial overlapping between SDFs and DF > 0.3 OI, HDF, and Rotors for all patients. Since the 2D density map is representing the entire LA, the overlapping results consider the entire size of LA.

4. Conclusions.

For all PersAF drivers tested, as time duration increases, the similarity and spatial overlapping of individual density maps improve. Therefore, our results suggest that using non-contact VEGMs, 60 s segment seems to be sufficient to identify important PersAF drivers. There is spatial overlapping between PersAF drivers density maps. Thereby, our results indicate that the different markers converged to similar regions as PersAF drivers, reinforcing that such regions are important for AF perpetuation. Furthermore, investigate regions of overlapping might lead to better identification of substrate targets ablation for PersAF.

Acknowledgments

References

[1] A. Chugh, Mapping and ablation of post-AF atrial tachycardias, J Cardiovasc Electrophysiol (2021).

[2] K. Nademanee, J. McKenzie, E. Kosar, M. Schwab, B. Sunsaneewitayakul, T. Vasavakul, C. Khunnawat, T. Ngarmukos, A new approach for catheter ablation of atrial fibrillation: mapping of the electrophysiologic substrate, Journal of the American College of Cardiology 43(11) (2004) 2044-2053.

[3] S.M. Narayan, D.E. Krummen, K. Shivkumar, P. Clopton, W.-J. Rappel, J.M. Miller, Treatment of atrial fibrillation by the ablation of localized sources: CONFIRM (Conventional Ablation for Atrial Fibrillation With or Without Focal Impulse and Rotor Modulation) trial, Journal of the American College of Cardiology 60(7) (2012) 628-636.

[4] J.A. Zaman, W.H. Sauer, M.I. Alhusseini, T. Baykaner, R.T. Borne, C.A. Kowalewski, S. Busch, P.C. Zei, S. Park, M.N. Viswanathan, Identification and characterization of sites where persistent atrial fibrillation is terminated by localized ablation, Circulation: Arrhythmia and Electrophysiology 11(1) (2018) e005258.

[5] Y.-J. Lin, M.-T. Lo, S.-L. Chang, L.-W. Lo, Y.-F. Hu, T.-F. Chao, F.-P. Chung, J.-N. Liao, C.-Y. Lin, H.-Y. Kuo, Benefits of atrial substrate modification guided by electrogram similarity and phase mapping techniques to eliminate rotors and focal sources versus conventional defragmentation in persistent atrial fibrillation, JACC: Clinical Electrophysiology 2(6) (2016) 667-678.

[6] M. Haissaguerre, M. Hocini, A. Denis, A.J. Shah, Y. Komatsu, S. Yamashita, M. Daly, S. Amraoui, S. Zellerhoff, M.-Q. Picat, Driver domains in persistent atrial fibrillation, Circulation 130(7) (2014) 530-538.

[7] S.M. Narayan, D.E. Krummen, W.J. RAPPEL, Clinical mapping approach to diagnose electrical rotors and focal impulse sources for human atrial fibrillation, Journal of cardiovascular electrophysiology 23(5) (2012) 447-454.

[8] S.M. Narayan, T. Baykaner, P. Clopton, A. Schricker, G.G. Lalani, D.E. Krummen, K. Shivkumar, J.M. Miller, Ablation of the rotor and focal sources reduces late recurrence of atrial fibrillation compared with trigger ablation alone: extended follow-up of the CONFIRM trial (Conventional Ablation for Atrial Fibrillation With or Without Focal Impulse and Rotor Modulation), Journal of the American College of Cardiology 63(17) (2014) 1761-1768.

[9] A. Kimata, Y. Yokoyama, S. Aita, H. Nakamura, K. Higuchi, Y. Tanaka, A. Nogami, K. Hirao, K. Aonuma, Temporally stable frequency mapping using continuous wavelet transform analysis in patients with persistent atrial fibrillation, Journal of cardiovascular electrophysiology 29(4) (2018) 514-522.

[10] J.L. Salinet, J.H. Tuan, A.J. Sandilands, P.J. Stafford, F.S. Schlindwein, G.A. Ng, Distinctive patterns of dominant frequency trajectory behavior in drug-refractory persistent atrial fibrillation: preliminary characterization of spatiotemporal instability, Journal of cardiovascular electrophysiology 25(4) (2014) 371-379.

[11] Xin. Li, G.S. Chu, T.P. Almeida, F.J. Vanheusden, J. Salinet, N. Dastagir, A.R. Mistry, Z. Vali, B. Sidhu, P.J. Stafford, F.S. Schlindwein and G. André Ng, Automatic Extraction of Recurrent Patterns of High Dominant Frequency Mapping During Human Persistent Atrial Fibrillation, Frontiers in Physiology 12 (2021).

[12] J.W. Jarman, T. Wong, P. Kojodjojo, H. Spohr, J.E. Davies, M. Roughton, D.P. Francis, P. Kanagaratnam, V. Markides, D.W. Davies, Spatiotemporal behavior of high dominant frequency during paroxysmal and persistent atrial fibrillation in the human left atrium, Circulation: Arrhythmia and Electrophysiology 5(4) (2012) 650-658.

[13] L. Roten, M. Pedersen, P. Pascale, A. Shah, S. Eliautou, D. Scherr, F. Sacher, M. Haïssaguerre, Noninvasive electrocardiographic mapping for prediction of tachycardia mechanism and origin of atrial tachycardia following bilateral pulmonary transplantation, Journal of cardiovascular electrophysiology 23(5) (2012) 553-555.

[14] R. Kogawa, Y. Okumura, I. Watanabe, M. Kofune, K. Nagashima, H. Mano, K. Sonoda, N. Sasaki, K. Ohkubo, T. Nakai, Spatial and temporal variability of the complex fractionated atrial electrogram activity and dominant frequency in human atrial fibrillation, Journal of arrhythmia 31(2) (2015) 101-107.

[15] J.L. Salinet Jr, J.P. Madeiro, P.C. Cortez, P.J. Stafford, G.A. Ng, F.S. Schlindwein, Analysis of QRS-T subtraction in unipolar atrial fibrillation electrograms, Medical & biological engineering & computing 51(12) (2013) 1381-1391.

[16] F.J. Vanheusden, G.S. Chu, X. Li, J. Salinet, T.P. Almeida, N. Dastagir, P.J. Stafford, G.A. Ng, F.S. Schlindwein, Systematic differences of non-invasive dominant frequency estimation compared to invasive dominant frequency estimation in atrial fibrillation, Computers in biology and medicine 104 (2019) 299-309.

[17] Xin. Li, T.P. Almeida, N. Dastagir, M.S. Guillem, J. Salinet, G.S. Chu, P.J. Stafford, F.S. Schlindwein, G.A. Ng, Standardizing single-frame phase singularity identification algorithms and parameters in phase mapping during human atrial fibrillation, Frontiers in physiology 11 (2020) 869.

[18] M. Ehnesh, Xin. Li, N. Dastagir, S. Ahmad, T.A. Biala, P.J. Stafford, G.A. Ng, F.S. Schlindwein, Investigating the Optimal Recording Duration for Summarising Spatiotemporal Behaviours of Long Lifespan Rotors Using Phase Mapping of Non-Contact Electrograms During Persistent Atrial Fibrillation, 2019 Computing in Cardiology (CinC), IEEE, 2019, pp. 1-4.

Address for correspondence:

Mahmoud Ehnesh
School of Engineering,
University of Leicester
University Road, Leicester LE1 7RH
me196@leicester.ac.uk